Published in final edited form as:
J Neurochem. 2010 May ; 113(4): 978–989. doi:10.1111/j.1471-4159.2010.06661.x.

Increased expression of cholesterol 24S-hydroxylase results in disruption of glial glutamate transporter EAAT2 association with lipid rafts: a potential role in Alzheimer's disease

Guilian Tian[*], **Qiongman Kong**[*], **Liching Lai**[*], **Abhik Ray-Chaudhury**[+], and **Chien-liang Glenn Lin**[*]

[*]Department of Neuroscience, The Ohio State University, Columbus, OH 43210, USA

[+]Department of Pathology, The Ohio State University, Columbus, OH 43210, USA

Abstract

The glial glutamate transporter EAAT2 is the major mediator of glutamate clearance that terminates glutamate-mediated neurotransmission. Loss of EAAT2 and associated glutamate uptake function has been reported in the brains of patients with Alzheimer's disease (AD). We previously reported that EAAT2 is associated with lipid raft microdomains of the plasma membrane. In the present study, we demonstrated that association of EAAT2 with lipid rafts is disrupted in AD brains. This abnormality is not a consequence of neuron degeneration, oxidative stress, or amyloid beta toxicity. In AD brains, cholesterol 24S-hydroxylase (CYP46), a key enzyme in maintenance of cholesterol homeostasis in the brain, is markedly increased in astrocytes but decreased in neurons. We demonstrated that increased expression of CYP46 in primary astrocytes results in a reduction of membrane cholesterol levels and leads to the dissociation of EAAT2 from lipid rafts and the loss of EAAT2 and associated glutamate uptake function. These results suggest that a disturbance of cholesterol metabolism may contribute to loss of EAAT2 in AD.

Keywords

glutamate transporter EAAT2; lipid raft microdomain; Alzheimer's disease; cholesterol 24S-hydroxylase; excitotoxicity

Introduction

A consensus definition of lipid rafts emerging from the Keystone Symposium of Lipid Rafts is: "Membrane rafts are small (10–200 nm), heterogeneous, highly dynamic, sterol- and sphingolipid-enriched domains that compartmentalize cellular processes. Small rafts can sometimes be stabilized to form larger platforms through protein-protein and protein-lipid interactions" (Pike 2006). Several kinds of neurotransmitter transporters have been reported to be localized in lipid rafts including γ-aminobutyric acid (GABA) transporter, 5-hydroxytryptamine (5-HT) transporter and glutamate transporters (Allen *et al.* 2007).

Excitatory amino acid transporter 2 (EAAT2) is the major glutamate transporter in the central nervous system. We previously reported that a large portion of total EAAT2 protein is associated with cholesterol-rich lipid raft microdomains of the plasma membrane. This

Address correspondence and reprint requests to Chien-liang Glenn Lin, 4198 Graves Hall, 333 W. 10th Avenue, Columbus, OH 43210, USA, lin.492@osu.edu.

association with lipid rafts is important for EAAT2 trafficking and function (Butchbach *et al.* 2004). In this report, we showed that depletion of membrane cholesterol by methyl-β-cyclodextrin resulted in a significant reduction of EAAT2 glutamate uptake activity. Cell surface biotinylation and immunostaining experiments revealed that the loss of cholesterol significantly altered the trafficking of EAAT2 to the plasma membrane as well as their membrane distribution, resulting in loss of EAAT2 protein (Butchbach *et al.* 2004). Similar observations were also reported by other groups (Zschocke *et al.* 2005).

Alzheimer's disease (AD), the most common form of dementia for the older population, is characterized by progressive cognitive deterioration in accordance with declining activities of daily living. Cholesterol metabolism has been proven to be an important element in AD risk and pathogenesis. A cluster of cholesterol-related genes have been reported to be associated with AD. Cholesterol 24S-hydroxylase (CYP46) mediates the conversion of cholesterol to 24S-hydroxycholesterol, which is a mechanism of the elimination of excess cholesterol and maintenance of cholesterol homeostasis in the brain (Bjorkhem *et al.* 1997, Lutjohann *et al.* 1996). It has been shown that the level of 24S-hydroxycholesterol is significantly increased in the serum and cerebrospinal fluid (CSF) of AD patients at the early stage of the disease (Lutjohann *et al.* 2000, Papassotiropoulos *et al.* 2002). In AD brains, CYP46 is markedly increased in astrocytes but decreased in neurons (Bogdanovic *et al.* 2001). These results suggest that more cholesterol is converted to 24S-hydoxycholesterol in AD brains. Furthermore, a recent study shows that the presence of the "T" allele in the polymorphic site rs754203 of the *CYP46* gene increases the risk of suffering from late-onset AD in person carrying the Apoε3 allele (Fernandez Del Pozo *et al.* 2006).

Several reports have demonstrated, through measurements of glutamate uptake and sodium-dependent glutamate binding, that the high affinity glutamate uptake system is impaired in AD brains (Cross *et al.* 1987, Hardy *et al.* 1987, Cowburn *et al.* 1988, Procter *et al.* 1988, Simpson *et al.* 1988, Chalmers *et al.* 1990, Scott *et al.* 1995, Masliah *et al.* 1996, Li *et al.* 1997). A malfunction in the glutamate uptake system can lead to the accumulation of excessive glutamate in the synapse, which is harmful to neurons. It has been shown that decreased glutamate transport activity is associated with decreased EAAT2 protein expression, but EAAT2 mRNA level is not affected (Li *et al.* 1997), suggesting that alterations in EAAT2 expression occur due to disturbances at the post-transcriptional level. Furthermore, Jacob *et al.* (2007) recently also reported marked impairment in the expression of EAAT2 at both gene and protein levels in AD brains (Jacob *et al.* 2007). Controversially, there are a few studies demonstrating no clear change in glutamate uptake and EAAT2 protein level in AD brains (McGeer *et al.* 1987, Rothstein *et al.* 1992, Rothstein *et al.* 1995, Beckstrom *et al.* 1999).

It has been reported that the organization of lipid rafts is disrupted in AD brains and this disruption is probably due to membrane cholesterol reduction (Ledesma *et al.* 2003). In the present study, we investigated whether association of EAAT2 with lipid raft microdomains is disrupted in AD brains. We found that the amount of EAAT2 associated with lipid rafts in AD brains was less than half of that in normal brains. We then investigated the cause of this abnormality and discovered that increased expression of CYP46 could result in dissociation of EAAT2 from lipid raft microdomains, which consequently caused loss of EAAT2 protein and associated glutamate uptake function.

Materials and methods

Post-mortem tissue

Frozen post-mortem brain tissues were provided by Harvard Brain Tissue Resource Center, Johns Hopkins Alzheimer's Disease Research Center Brain Bank, and University of

Maryland Brain and Tissue Banks for Developmental Disorders. The CERAD (Consortium to Establish a Registry for Alzheimer's Disease) criteria were used for diagnostic categorization of AD (Mirra *et al.* 1991). AD brain tissues were obtained from AD patients in the moderate or severe stages of Alzheimer's. No other significant gross or microscopic abnormalities were present in these AD brains. Control brain tissues were obtained from subjects who had no history of dementia and no evidence of significant neuropathological changes. The causes of death for these control subjects include arteriosclerotic cardiovascular disease, congenital heart disease, asthma, and renal failure. Specimens from Brodmann areas 9 and 10 in the frontal cortex were studied. Tissues were frozen using isopentane/dry ice and then stored at −80°C until use.

For the immunohistochemical study, the formalin-fixed, paraffin-embedded tissues were provided by Ohio State Brain Bank. AD brain tissues were obtained from AD patients in the severe stages of Alzheimer's. Control brain tissues were obtained from patients having pathology outside the CNS. The causes of death include heart failure, respiratory failure, renal failure, liver failure, and malignancy. The patient information for these post-mortem brain tissues is shown in supplementary Table 1.

Lipid raft microdomain preparation

The cholesterol-rich lipid raft microdomains were isolated as described previously with minor revision based on different samples (Butchbach *et al.* 2004). At the beginning of this study, we compared total membranes and plasma membranes for lipid raft preparation and did not observe any difference. We therefore used total membranes for the entire study. For post-mortem tissues, 100–200 mg frozen tissues were homogenized in 10 volumes of buffer A (150 mM NaCl, complete protease inhibitor cocktail (Roche Applied Science, Indianapolis, IN, USA), 100 μM phenylmethylsulfonyl fluoride (Sigma, St. Louis, MO, USA), in 25 mM MES, pH 6.5) using a Dounce homogenizer (30 passes with a type B pestle) followed by a 22-gauge needle (5 passes). The homogenates were centrifuged at 1,000 ×g for 10 min at 4°C, and the supernatants were diluted to 3 mg/ml protein and then incubated with 1% (v/v) Brij-58 (Sigma, St. Louis, MO, USA) for 60 min at 4°C, after which equal volume of 80% (w/v) sucrose was added to the samples to give a final concentration of 40% (w/v). 1 ml of each sample was overlaid with 1.8 ml of 30% (w/v) sucrose followed by 1.2 ml of 5% (w/v) sucrose and centrifuged for 16 hrs at 175,587 ×g at 4 °C using a SW60 rotor and a L8-M ultracentrifuge. Ten 400-μl fractions were taken from each sample.

For primary astrocyte and primary cortical culture, cells were scraped off in 1× PBS and centrifuged for 10 min at 1,000 ×g at 4°C. The pellets were sonicated in buffer A and then diluted to 3 mg/ml protein and incubated with 1% (v/v) Brij-58 for 60 min at 4°C. The homogenates were centrifuged at 1, 000 ×g for 10 min at 4°C, and supernatants were added with equal volume of 80% (w/v) sucrose. 1 ml of each sample was overlaid with 1.8 ml of 30% (w/v) sucrose followed by 1.2 ml of 5% (w/v) sucrose and centrifuged for 16 hrs at 175,587 ×g at 4 °C.

Immunoblot analysis

Immunoblotting was performed as described previously (Guo *et al.* 2002). In brief, the harvested samples were sonicated in 1× PBS containing complete protease inhibitor cocktail, assayed for protein concentration, resolved by SDS-PAGE (8% PA) and transferred onto PVDF membranes. The following primary antibodies were used: rabbit polyclonal antibodies (1:4000) against the C-terminus of human EAAT2 (position 553–568), rabbit anti-CYP46 polyclonal antibodies (1:400; Invitrogen), rabbit anti-caveolin polyclonal antibodies (1:1000; Santa Cruz, CA, USA), mouse anti-flotillin monoclonal antibodies

(1:500, B&D Laboratory, NJ, USA), and goat anti-actin polyclonal antibodies (1:2000; Santa Cruz Biotechnology, CA, USA). The immunoreactive bands were detected using the SuperSignal West Pico Chemiluminescent Substrate (Pierce Biotechnology, Rockford, IL, USA) according to manufacturer's directions. Band intensities were analyzed with ImageJ software.

For the analysis of EAAT2 distribution in the lipid raft fractions (Figs. 1C, 2C, 4B, and supplementary Figs. 1C, 2C, 3D), each Western blot was analyzed separately. For each Western blot, we determined "% of EAAT2 in the lipid raft fractions" by dividing the sum of EAAT2 signal intensities from fractions 3, 4, and 5 by the sum of total EAAT2 signal intensities (fractions 1 to 10). For Figs. 2A, 3C, and supplementary Figs. 1A, 2A, 3B, each study was repeated 3–4 times. All samples for each study were run on one Western blot. The mean of the signal intensities of all control samples was used to determine the value of "% of control".

Cell cultures

Mouse primary cortical cultures were obtained as described previously (Guo *et al.* 2003). In brief, cortices were dissected out of the newborn (P0–P1) brains and incubated in activated papain for 30 min at 37°C, triturated by repeated pipetting with a small bore pipette and plated onto poly-D-lysine (0.1 mg/ml; Sigma, St. Louis, MO, USA)-coated plastic culture dishes or glass slides. These cultures were maintained in Dulbecco's modified Eagle media (DMEM, Invitrogen, Carlsbad, CA, USA) containing 25 mM glucose, 1 mM sodium pyruvate, 19.4 μM pyridoxine hydrochloride, 2 mM glutamine and 1% B-27 supplement (Invitrogen, Carlsbad, CA, USA).

Rat primary astrocyte cultures were obtained from Dr. Richard W. Burry (Department of Neuroscience, The Ohio State University). The cells were maintained in DMEM with 10% fetal bovine serum (FBS; Invitrogen, Carlsbad, CA, USA).

Aβ1–42 treatment

Lyophilized and HPLC-purified amyloid beta peptide (Aβ1–42) was purchased from AnaSpec, Inc. (San Jose, CA, USA) and prepared following the manufacturer's instructions. In brief, 3 mM Aβ1–42 stock solutions were prepared in 1% NH_4OH as stock solution. It was then diluted with PBS and incubated at 37°C for 72 hrs to generate aggregated amyloid. Aβ1–42 oligomers at a final concentration of 1 μM were applied in all experiments.

Animal models

All animal experiments were performed at Ohio State University under national and institutional guidelines using protocols approved by the the Animal Care & Use Committee of Ohio State University. Human $SOD1^{G93A}$ transgenic mice (B6SJL-Tg [SOD1-G93A] 1Gur with high copy number of the mutant human SOD1 gene) were purchased from Jackson Laboratory (Bar Harbor, ME, USA). Adult same gender mice were housed 5 per cage, under 12 hr dark/light cycles. $APP_{Sw,Ind}$ transgenic mice were obtained from the laboratory of Dr. Lennart Mucke of the J. David Gladstone Institutes of San Francisco, CA. Transgene was determined by PCR using genomic DNA extracted from tail biopsies.

Mouse CYP46 cDNA cloning

Mouse brain total RNA was isolated with TRIzol (Invitrogen, Carlsbad, CA, USA) and first-strand cDNA was synthesized with Thermoscript reverse transcriptase (Invitrogen, Carlsbad, CA, USA) using an CYP46-specific primer (5′-TCCAAGGAGTCTGACCTTACCCA-3′). Primer set (5′-TCCAAGGAGTCTGACCTTACCCA-3′ and 5′-AGCTAGTCGGTCGCAGCCTC-3′) was used for PCR reaction and PCR product was

cloned into pPCR-ScriptAmpSK(+) (Stratagene, La Jolla, CA, USA) and then subcloned into pcDNA3 with *EcoR* I and *Not* I to generate pcDNA3-CYP46.

To generate pcDNA4-CYP46, PCR primer set (5′-GAATTCTGCCGACCACGAGCCATGAGC-3′ and 5′-AGTCTGACCTTACCCAGGGCTCA-3′) was employed to amplify CYP46 using pcDNA3-CYP46 as template, and the PCR product was cloned into pPCR-ScriptAmpSK(+) and then subcloned into pcDNA4 with *EcoR* I.

Generation of stably transfected primary astrocyte cell lines

The generation of a primary astrocyte line stably expresses EAAT2 was described previously (Tian *et al.* 2007). In brief, low passage (4 passages) rat primary astrocytes were transfected with pcDNA3/EAAT2 and the medium was replaced with fresh medium containing geneticin (0.9 mg/ml) 48 hrs post-transfection to select for EAAT2-expressing cells. Selected colonies were examined for EAAT2 expression by RT-PCR using EAAT2 specific primers and also by immunoblotting using rabbit anti-EAAT2 polyclonal antibodies. This cell line was named as PA-EAAT2.

To generate a primary astrocyte cell line stably expressing both EAAT2 and CYP46, low passage PA-EAAT2 cells were plated onto cell culture dishes and transfected with pcDNA4/CYP46 using Expression Fect (ISC BioExpress, Kaysville, UT, USA) according to standard protocol. The medium was replaced with fresh medium containing Zerocin (400 mg/ml) 48 hrs post-transfection to select for CYP46-expressing cells. Selection medium was replaced every 3 days until colonies formed (18–21 days later). Colonies were examined for CYP46 expression by RT-PCR using CYP46 specific primers. This cell line was named as PA-EAAT2-CYP.

Quantitative RT-PCR

Total RNA from primary astrocytes or primary cortical cultures was isolated with TRIzol (Invitrogen, Carlsbad, CA, USA) and first-strand cDNA was synthesized with M-MLV reverse transcriptase (Invitrogen, Carlsbad, CA, USA) using a mouse CYP46-specific primer (5′-GAATTCTGCCGACCACGAGCCATGAGC-3′) and an EAAT2 specific primer (5′-ACGCTGGGGAGTTTATTCAAGAAT-3′). β-actin was used as an internal control (primer: 5′-TGTCAAAGAAAGGGTGTAAAACGCAGC-3′). PCR primers (5′-TCCTGCATCGGCCAACAGTTTGCTCAG-3′ and 5′-GAATTCTGCCGACCACGAGCCATGAGC-3′) were used for CYP46 cDNA, PCR primers (5′-GGCAACTGGGGATGTACA-3′ and 5′-ACGCTGGGGAGTTTATTCAAGAAT-3′) were used for EAAT2 cDNA and primers (5′-CGGGACCTGACAGACTACCTCAT-3′ and 5′-TGTCAAAGAAAGGGTGTAAAACGCAGC-3′) were used for actin cDNA. PCR condition were as follows: 95°C for 3 min, 85°C for 2 min; 95°C for 30 sec, 60°C for 30 sec, 72°C for 1 min for 30 cycles followed by 10 min extension at 72°C. Quantitative PCR analysis was done by running various numbers of PCR cycles and serial dilutions of RT product.

We also confirmed the results by real-time PCR. Real-time PCR was performed using SYBR GREEN PCR Master Mix (Applied Biosystems, Foster City, CA). PCR primers (5′-TAACTCTGGCGGCCAATGGAAAGT-3′ and 5′-ACGCTGGGGAGTTTATTCAAGAAT-3′) were used for EAAT2 cDNA and primers (5′-TGGATCAGCAAGCAGGAGTACGA-3′ and 5′-TGTCAAAGAAAGGGTGTAAAACGCAGC-3′) were used for actin cDNA. PCR conditions were as follows: 95°C for 10 min; 95°C for 15 sec, 60°C for 1 min for 40 cycles.

[^{3}H]glutamate uptake assay

Uptake of radiolabeled glutamate was monitored in cultured cells as described previously with minor change (Tian *et al.* 2007). In brief, cultured cells grown on 24-well plates were washed with uptake sample buffer (320 mM sucrose in 50 mM TrisHCl, pH 7.4) and then incubated for 10 min at 37°C with L-[^{3}H]glutamate (0.1 μCi; Amersham Biosciences, Piscataway, NJ, USA) in either Na^+-containing or Na^+-free Kreb's buffer supplemented with unlabelled glutamate to achieve final concentration of 2–200 μM. The cells were washed with ice-cold 1× PBS and lysed in 1 mM NaOH. The amount of radiolabeled glutamate was measured using a Beckman Coulter LS6500 Multi-Purpose Scintillation Counter (Beckman Coulter, Fullerton, CA, USA). Na^+-dependent L-[^{3}H]glutamate uptake was calculated by subtracting Na^+-independent L-[^{3}H]glutamate uptake (in Na^+-free Kreb's buffer) from the total L-[^{3}H]glutamate uptake (in Na^+-containing Kreb's buffer).

Cholesterol assay

Cells were lysed in reaction buffer (5 mM cholic acid, 0.1% Triton X-100 in PBS, pH 7.4) for 30 min at 4°C and then sonicated. Membrane cholesterol was measured using the Amplex Red Cholesterol Assay kit (Invitrogen, Carlsbad, CA, USA) according to manufacturer's directions except that cholesterol esterase was omitted from the reaction mixture. Fluorescence was measured with a GENios microplate reader (Tecan Company; λ_{ex}=545 nm, λ_{em}=610 nm). The protein concentrations of the samples were determined using Coomassie Plus Protein Assay according to manufacturer's directions. Membrane cholesterol levels were expressed as specific fluorescence/mg protein.

Transfection

Primary astrocyte cells were plated on six-well plates at a density of 1×10^6 cells per well and allowed to adhere overnight. For each well, 1 μg of plasmid DNA (pcDNA3-EGFP and pcDNA3-CYP46) and 2 μl Expression Fect (ISC BioExpress, Kaysville, UT, USA) were diluted into 100 μl of DMEM respectively, and then Expression Fect solution was added into DNA solution. The mixture was incubated at room temperature for 20 min and was added to 2 ml serum-containing medium in each well. The transfected cells were harvested for analysis after incubation at 37°C for 72 hrs. For primary cortical culture, the transfection was done on day 7 using the same procedure described above.

Immunohistochemistry

Paraffin-embedded sections were cut at 10 μm for immunofluorescent staining. Sections were deparaffinized in xylene (5 min, 3×) and rehydrated through alcohols to water (100% ethanol for 3 min (2×), 95% ethanol for 1 min (1×), 75% ethanol for 3 min (1×)). High temperature antigen retrieval was performed in a 90°C water bath using 2.5% citric acid (pH 6.0) for 30 min. Nonspecific sites were blocked using blocking solution (10% normal goat serum/0.5% BSA in PBST (0.025% Triton X-100 in PBS)) for 1 hr at room temperature followed by addition of the primary antibodies and incubation for overnight at 4°C. The following antibodies were used: rabbit anti-GFAP polyclonal antibodies (1:1000, Promega, Madison, WI, USA), mouse anti-CYP monoclonal antibodies (Neat hybridoma culture supernatants supplemented with Triton X-100 to 0.025%; Ramirez *et al.* 2008)), rabbit anti-CYP46 polyclonal antibodies (1:200; Invitrogen), rabbit anti-EAAT2 polyclonal antibodies (1:200). After rinsing with PBST (10 min, 3×), the slides were then incubated with secondary antibody solution (Alexa Fluor 488 goat anti-rabbit IgG (1:1000), Alexa Fluor 594 goat anti-mouse IgG (1:1000), or Hoechst 33342 in blocking solution) at room temperature for 1 hr. The slides were then rinsed with PBST (10 min, 3×) and mount with immumount. The images were obtained from an Axioskop 2 (Carl Zeiss) inverted microscopy and the signal intensities were analyzed with ImageJ software.

Statistical analysis

The quantitative data in this study were expressed as the mean ± SEM. For Figs. 1C, 2C, 4B and supplementary Figs. 1C, 2C, 3D, Wilcoxon rank-sum test was used to determine the significance of difference. For Fig. 5B, a linear mixed effects model was constructed with a random effect that was used to adjust for the within-subject correlation in the repeated measures for each subject. Student's t-test was performed for the rest of data when the normality assumption was found to be reasonable.

Results

The association of EAAT2 with lipid rafts is partially disrupted in AD frontal cortices

The frontal cortex of AD brains (n=11) and age-matched normal brains (n=6) were used in this study. The total EAAT2 protein levels in theses AD tissues were significantly lower than that in the normal tissues (Fig. 1A). These results were consistent with previous reports (Li *et al.* 1997). We investigated whether EAAT2 proteins are properly associated with lipid raft microdomains of the plasma membrane in AD brains. Tissues were homogenized, solubilized with 1% Brij-58 and fractionated through a discontinuous sucrose gradient. The detergent-resistant microdomains (lipid rafts) and their associated proteins migrated to the upper, low density region of the gradient, while the detergent-soluble materials (non-lipid rafts) remained in the lower, high density fractions. The fractions were collected from the top of the gradient (fraction 1–11). Flotillin-1, which is known to be associated with lipid raft, was localized to fractions 3–5, indicating that these fractions contained lipid raft microdomains. For normal brain samples, a large portion of total EAAT2 protein was detected in lipid raft fractions (fraction 3–5); however, for AD brain samples, less EAAT2 protein was localized in lipid raft fractions and more EAAT2 protein was detected in non-lipid raft fractions (fraction 8–10) (Fig. 1B). Statistical analysis revealed a significant decrease in the association of EAAT2 protein with lipid raft microdomains in AD frontal cortices (35.4±9.6% of total EAAT2 protein) compared to normal controls (74.2±4.7% of total EAAT2 protein) (Fig. 1C). The post-mortem interval did not affect the amount of EAAT2 protein associated with lipid raft microdomains (Fig. 1D). However, several lipid raft associated proteins, including flotillin-1, caveolin and prion protein (PrP), were primarily localized in lipid raft fractions in AD samples, similarly seen in normal control samples (Fig. 1B). These results indicated that the association of EAAT2 with lipid rafts is specifically disrupted in AD frontal cortices.

Neuronal death is not the cause of dissociation of EAAT2 from lipid raft microdomains

What could be the cause of dissociation of EAAT2 from lipid raft microdomains in AD brains? We investigated whether dissociation of EAAT2 from lipid raft microdomains is the consequence of neuron degeneration. Transgenic mice expressing familial amyotrophic lateral sclerosis (ALS)-linked mutant copper-zinc superoxide dismutase ($SOD1^{G93A}$) develop similar clinical and pathological phenotypes as seen in ALS patients. These mice begin to lose motor neurons at about 90 days of age and eventually die at about 120–140 days of age. The EAAT2 protein levels decreased as disease progresses. At 120 days of age, there was a 60–80% loss of EAAT2 protein in the lumbar spinal cords (supplementary Fig. 1A). We performed lipid raft preparation in the lumbar spinal cords of 120 day-old $SOD1^{G93A}$ transgenic mice in which majority of motor neurons were degenerated. The lumbar spinal cords of non-transgenic littermates were the controls. The results showed that the distribution of EAAT2 in lipid raft and non-lipid raft fractions were similar between $SOD1^{G93A}$ transgenic and non-transgenic samples (supplementary Fig. 1B). A majority of total EAAT2 protein (~80%) was enriched in lipid rafts and only a small portion of EAAT2 (~20%) was localized in non-lipid raft fractions (supplementary Fig. 1C). These results

indicated that neuronal death is not the cause of dissociation of EAAT2 from lipid raft microdomains.

Oxidative stress and amyloid β peptide do not affect the association of EAAT2 with lipid rafts

We investigated whether oxidative stress could cause dissociation of EAAT2 from lipid raft microdomains. Mouse primary cortical neurons and astrocytes mixed cultures prepared from neonatal (P0–P1) wild-type mouse pups were used in this study. The cultures contained ~50% neurons and ~50% astrocytes including type II astrocytes, which express EAAT2. The cultures were treated with 50 μM H_2O_2 in DMEM for 30 minutes, which caused significant oxidative damage (Shan *et al.* 2007), and then harvested at 4 hours post-treatment for lipid raft preparation. The results showed that there was no significant difference in the distribution of EAAT2 in lipid raft and non-lipid raft fractions between H_2O_2-treated and non-treated cells (supplementary Fig. 2B&C), suggesting that oxidative stress induced by H_2O_2 does not affect the association of EAAT2 with lipid rafts.

We further investigated whether amyloid β peptide (Aβ) could cause EAAT2 dissociated from lipid raft microdomains. The primary cortical neurons and astrocytes mixed cultures were treated with 1 μM of Aβ1–42 in DMEM for 48 hours, which caused significant cytotoxicity (Shan *et al*. 2007). The cultures were then harvested for lipid raft preparation. The results showed that the amounts of EAAT2 associated with lipid rafts microdomains were similar between Aβ1–42-treated and non-treated cells (supplementary Fig. 2B&C), suggesting that Aβ may not affect the association of EAAT2 with lipid rafts.

Furthermore, we examined whether abnormal APP process could affect association of EAAT2 with lipid raft microdomains. $APP_{Sw,Ind}$ transgenic mice, which express human APP bearing both the Indiana (V717F) and the Swedish (K670N/M671L) mutations (Mucke *et al.* 2000), were used in this study. These mice exhibit onset of Aβ plaques, loss of synaptic density, and loss of memory beginning from the age of 6–8 months. The intracellular Aβ load is detectable at the age of 3 months (Galvan *et al.* 2006). The mice begin to lose EAAT2 protein at ~4–5 months of age and EAAT2 protein levels gradually decrease as disease progresses (Fig. 2A shows the results of 9-month-old samples). We performed lipid raft preparation on the forebrains of different ages of $APP_{Sw,Ind}$ transgenic mice, including 3-, 6- and 9-month-old. The forebrains of non-transgenic littermates were the controls. There was no significant difference in EAAT2 distribution between $APP_{Sw,Ind}$ transgenic and non-transgenic samples (Fig. 2B&C shows the results of 9-month-old samples). These results indicated that abnormal APP process and amyloid deposition do not induce dissociation of EAAT2 from lipid rafts.

Up-regulation of CYP46 causes dissociation of EAAT2 from lipid raft microdomains and decrease of EAAT2 protein level and glutamate uptake

Cholesterol 24S-hydroxylase (CYP46) is a key enzyme in maintenance of cholesterol homeostasis in the brain. It has been reported that in AD brains, CYP46 is increased in astrocytes but decreased in neurons (Bogdanovic *et al*. 2001). We tested whether up-regulation of CYP46 could cause dissociation of EAAT2 from lipid raft microdomains. We first cloned mouse CYP46 cDNA and established two primary astrocyte cell lines: one cell line stably expressing EAAT2 (named as PA-EAAT2) and the other cell line expressing both EAAT2 and CYP46 (named as PA-EAAT2-CYP). Quantitative RT-PCR analysis revealed that PA-EAAT2-CYP cells expressed greater amounts of CYP46 mRNA than that of PA-EAAT2 cells (Fig. 3A), but both cell lines expressed similar amounts of EAAT2 mRNA (Fig. 3B). Interestingly, PA-EAAT2-CYP cells expressed significantly smaller amounts of EAAT2 protein (~40–50% fewer) than that of PA-EAAT2 cells (Fig. 3C).

Consistently, [^{3}H]glutamate uptake activity in PA-EAAT2-CYP cells was significantly decreased when compared to that in PA-EAAT2 cells (Fig. 3D). Increased CYP46 expression caused a decrease in uptake *V*max and an increase in the apparent glutamate *K*m.

We then examined EAAT2 lipid raft microdomain localization in these cell lines. The results showed that the amount of EAAT2 associated with lipid raft microdomain in PA-EAAT2-CYP cells (~50%) was significantly reduced compared to that in PA-EAAT2 cells (~80%) (Fig. 4A&B). However, the amount of flotillin-1 associated with lipid raft microdomain was similar between these two cell lines. Total cholesterol levels (Fig. 4C) as well as membrane cholesterol levels (Fig. 4D) were significantly decreased in PA-EAAT2-CYP cells when compared with that in PA-EAAT2 cells. These results suggest that increased CYP46 can cause reduction of membrane cholesterol levels, which consequently results in dissociation of EAAT2 from lipid raft microdomains and leads to a decrease in EAAT2 protein levels and associated glutamate uptake functions.

To further confirm the above results, we transfected pcDNA3-CYP46 cDNA into primary cortical neuron and astrocyte mixed cultures and pcDNA3-GFP cDNA was used as a control. The transfected cultures were harvested for RT-PCR, immunoblot and lipid raft analyses at 72 hours post-transfection. The cultures transfected with pcDNA3-CYP46 cDNA expressed higher level of CYP46 mRNA than the cultures transfected with pcDNA3-GFP cDNA, indicating that the exogenous CYP46 cDNA was properly expressed (supplementary Fig. 3A). Importantly, we observed that total EAAT2 protein levels in the cultures transfected with pcDNA3-CYP46 cDNA was much lower (~40–50%) than that in the cultures transfected with pcDNA3-GFP cDNA (supplementary Fig. 3B), but EAAT2 mRNA levels were similar (supplementary Fig. 3A). Moreover, about 20–30% of EAAT2 protein was shifted from the lipid raft fractions to the non-lipid raft fractions in the cultures transfected with pcDNA3-CYP46 cDNA, compared with the cultures transfected with pcDNA3-GFP cDNA (supplementary Fig. 3C&D). There was no obvious change for the flotillin distribution (supplementary Fig. 3C).

We further examined the relationship between CYP46 and EAAT2 in AD frontal cortices by immunohistochemistry. Consistent with previous report (Bogdanovic *et al.* 2001), we observed a significant increase in CYP46 immunoreactivity in the GFAP-positive astrocytes of AD frontal cortices when compared with normal controls (Fig. 5A&B). The results were confirmed by using two different sources of anti-CYP46 antibodies. Importantly, we observed that the increase of CYP46 immunoreactivity is concomitant with a focal loss of EAAT2 immunoreactivity in AD frontal cortices (Fig. 5C).

Taken together, the above results suggest that increased expression of CYP46 may be one of factors that causes dissociation of EAAT2 from lipid raft microdomains and loss of EAAT2 protein and associated glutamate uptake function in AD brains.

Discussion

In the present study, we demonstrated that the association of EAAT2 with lipid rafts is disrupted in AD frontal cortices. This abnormality may not be a consequence of neuron degeneration, oxidative stress, or amyloid beta toxicity. It may be partially due to up-regulation of CYP46. We determined that increased expression of CYP46 in primary astrocytes causes the reduction of membrane cholesterol levels and leads to EAAT2 dissociated from lipid rafts, which results in loss of EAAT2 protein and associated glutamate uptake function. Our data suggest that disturbance of cholesterol metabolism may contribute to loss of EAAT2 in AD.

The AD frontal cortex tissues used in this study had a 30–40% loss of EAAT2 (Fig. 1A). This result is consistent with two previous studies (Li *et al*. 1997,Jacob *et al*. 2007) but disagrees with other studies (Rothstein *et al*. 1992,Rothstein *et al*. 1995,Beckstrom *et al*. 1999). The loss of EAAT2 in AD tissues is not due to the postmortem delay because the normal control tissues have a similar, even slightly longer, postmortem delay (see supplementary Table 1). The anti-EAAT2 antibody used in this study is similar to that used in the studies of Rothstein *et al*. We think the controversy is potentially due to sample preparation and data analysis. EAAT2-positive astrocytes are not evenly distributed in the frontal cortex; even within the white matter, the density of EAAT2-positive astrocytes is variant in different regions. Therefore, we collected and combined different regions of the frontal cortex for analysis. In addition, it is critical to normalize the data to an astrocyte marker. However, it is difficult to find an appropriate astrocyte marker for this analysis because the expression levels of commonly used astrocyte markers, GFAP and glutamine synthetase, are changed in AD brains (Robinson 2001). We used glutamine synthetase to normalize EAAT2 protein levels because of the following reasons. We observed a slight, not marked, decrease of glutamine synthetase in some AD samples. If the results still show a decrease in EAAT2 protein levels in AD samples after normalizing to glutamine synthetase, it indicates that EAAT2 protein is indeed decreased in AD tissues. We also normalized EAAT2 protein levels to actin and the results indicated a loss of EAAT2 protein in AD samples. In addition, our immunohistochemical analysis also showed a loss of EAAT2 in AD frontal cortices (Fig. 5C).

EAAT2 proteins are normally associated with Brij58-resistant cholesterol-enriched microdomains of the plasma membrane, and this association is important for EAAT2 trafficking and function (Butchbach *et al*. 2004). In this study, we observed a significant decrease in the association of EAAT2 protein with Brij58-resistant lipid rafts in AD frontal cortex tissues (~40–50% decrease) when compared with age-matched normal controls (Fig. 1B&C). This abnormality is not due to the effects of post-mortem intervals (Fig. 1D). Whether agonal state of disease causes this abnormality is unknown. We examined cerebellum tissues (unaffected area) in the same AD patients and did not find any abnormality (data not shown); however, the cerebellum may not be an ideal control for "agonal state". The spared cortical area may be more suitable but is not available from brain banks.

Several lipid raft associated proteins, such as flotillin-1, were still associated with Brij58-resistant lipid rafts (Fig 1B). Why is EAAT2 affected but not other proteins? We previously demonstrated that EAAT2-associated lipid raft microdomains are soluble in Triton X-100 but insoluble in more hydrophilic nonionic detergents such as Brij58 and Lubrol WX (Butchbach *et al*. 2004). However, flotillin-1-associated lipid raft microdomains are insoluble in Triton X-100. This indicates that flotillin-1-associated lipid raft microdomains contain more cholesterol, which makes them resistant to Triton X-100 (a less hydrophilic nonionic detergent), but EAAT2-associated lipid raft microdomains contain relatively less cholesterol so they are only resistant to Brij58 (a more hydrophilic nonionic detergent). When the membrane cholesterol level is reduced, EAAT2-associated lipid raft microdomains are disrupted while flotillin-1-associated lipid raft microdomains are still resistant to Brij58.

It has been reported that plasmin, a serine protease which can degrade amyloid peptide, is dissociated from lipid rafts in AD brains, due to a significant reduction in plasma membrane cholesterol level (Ledesma *et al*. 2003). The authors demonstrated that lipid raft microdomains are anomalous in AD, which is reflected by lower levels of several lipid raft associated proteins, including the flotillin-1, the ganglioside GM1 and the urokinase-type plasminogen activator receptor (uPAR), localized in lipid raft fractions. It is possible that in

AD brains, the lipid rafts are no longer efficient as a mean of clustering proteins due to lower concentration of cholesterol present in the plasma membrane.

It is notable that in the lipid raft fractions EAAT2 shows monomeric and multimeric bands, whereas in the non-lipid raft fractions EAAT2 shows predominantly multimeric bands. It is possible that the non-raft components may be a reservoir where the oxidized and damaged EAAT2 accumulate, therefore, more multimeric EAAT2 were present in the non-lipid raft fractions (Haugeto *et al.* 1996, Trotti *et al.* 1998). The other potential explanation is that it may be simply due to the higher sucrose concentration in the non-lipid raft fractions, which prevents multimeric EAAT2 from breaking down to monomeric EAAT2 during sample preparation.

Amyloid β peptide has been reported to affect multiple aspects of cholesterol metabolism, including inhibiting cholesterol synthesis, inducing cholesterol oxidation and removing cholesterol form membrane (Grimm *et al*. 2005, Cutler et al. 2004, Michikawa *et al*. 2001). However, in this study, we did not observe the effect of Aβ1–42 on the association of EAAT2 with lipid rafts in primary cortical cultures (supplementary Fig. 2). In addition, EAAT2 is properly associated with lipid raft in $APP_{Sw,Ind}$ transgenic mice (Fig. 2). It is possible that the effect of amyloid β peptide on the organization of lipid rafts is not significant enough to be detected by the methods used in this study.

Many studies have demonstrated that CYP46 is associated with pathogenesis of AD (Wang & Jia 2007, Helisalmi *et al.* 2006, Johansson *et al.* 2004, Papassotiropoulos *et al*. 2003). In this study, we provided a new pathway to connect the abnormal cholesterol metabolism with AD pathogenesis. Up-regulation of CYP46 reduces the amount of cholesterol in the plasma membrane, which destabilizes the lipid raft microdomains. This could lead to dissociation of EAAT2 protein from lipid rafts. When EAAT2 is dissociated from lipid rafts, it may become unstable and degrade. The question as to what causes up-regulation of CYP46 remains to be explored.

The findings in this study indicate that increased expression of CYP46 may be one of the factors causing lipid raft disorganization in AD and suggest that other lipid rafts associated proteins may also be affected. It is well known that the association with lipid raft is critical for the normal function of many proteins including receptors and transporters. Therefore, the prevention of lipid raft disorganization may be an important therapeutic target for AD.

Supplementary Material

Refer to Web version on PubMed Central for supplementary material.

Acknowledgments

This work was supported by the NIH (grants MH59805 and NS64275) and the Alzheimer's Association. We thank Harvard Brain Tissue Resource Center, Johns Hopkins Alzheimer's Disease Research Center Brain Bank, and University of Maryland Brain and Tissue Banks for Developmental Disorders for providing AD and normal control brain tissues. We also thank Dr. David W. Russell (University of Texas Southestern Medical Center) for providing anti-CYP46 antibody, Dr. Lennart Mucke (Gladstone Institute of Neurological Disease, University of California, San Francisco) for providing $APP_{Sw,Ind}$ transgenic mice, and Dr. Xin He (University of Maryland, College Park) for assistance with statistical analysis.

References

Allen JA, Halverson-Tamboli RA, Rasenick MM. Lipid raft microdomains and neurotransmitter signalling. Nat Rev Neurosci. 2007; 8:128–140. [PubMed: 17195035]

Beckstrom H, Julsrud L, Haugeto O, Dewar D, Graham DI, Lehre KP, Storm-Mathisen J, Danbolt NC. Interindividual differences in the levels of the glutamate transporters GLAST and GLT, but no clear correlation with Alzheimer's disease. J Neurosci Res. 1999; 55:218–229. [PubMed: 9972824]

Bjorkhem I, Lutjohann D, Breuer O, Sakinis A, Wennmalm A. Importance of a novel oxidative mechanism for elimination of brain cholesterol. Turnover of cholesterol and 24(S)-hydroxycholesterol in rat brain as measured with 18O2 techniques in vivo and in vitro. J Biol Chem. 1997; 272:30178–30184. [PubMed: 9374499]

Bogdanovic N, Bretillon L, Lund EG, Diczfalusy U, Lannfelt L, Winblad B, Russell DW, Bjorkhem I. On the turnover of brain cholesterol in patients with Alzheimer's disease. Abnormal induction of the cholesterol-catabolic enzyme CYP46 in glial cells. Neurosci Lett. 2001; 314:45–48. [PubMed: 11698143]

Butchbach ME, Tian G, Guo H, Lin CL. Association of excitatory amino acid transporters, especially EAAT2, with cholesterol-rich lipid raft microdomains: importance for excitatory amino acid transporter localization and function. J Biol Chem. 2004; 279:34388–34396. [PubMed: 15187084]

Chalmers DT, Dewar D, Graham DI, Brooks DN, McCulloch J. Differential alterations of cortical glutamatergic binding sites in senile dementia of the Alzheimer type. Proc Natl Acad Sci U S A. 1990; 87:1352–1356. [PubMed: 2154742]

Cowburn R, Hardy J, Roberts P, Briggs R. Regional distribution of pre- and postsynaptic glutamatergic function in Alzheimer's disease. Brain Res. 1988; 452:403–407. [PubMed: 2900052]

Cross AJ, Slater P, Simpson M, Royston C, Deakin JF, Perry RH, Perry EK. Sodium dependent D-[3H]aspartate binding in cerebral cortex in patients with Alzheimer's and Parkinson's diseases. Neurosci Lett. 1987; 79:213–217. [PubMed: 2823192]

Cutler RG, Kelly J, Storie K, Pedersen WA, Tammara A, Hatanpaa K, Troncoso JC, Mattson MP. Involvement of oxidative stress-induced abnormalities in ceramide and cholesterol metabolism in brain aging and Alzheimer's disease. Proc Natl Acad Sci U S A. 2004; 101:2070–2075. [PubMed: 14970312]

Fernandez Del Pozo V, Alvarez Alvarez M, Fernandez Martinez M, Galdos Alcelay L, Gomez Busto F, Pena JA, Alfonso-Sanchez MA, Zarranz Imirizaldu JJ, de Pancorbo MM. Polymorphism in the cholesterol 24S-hydroxylase gene (CYP46A1) associated with the APOEpsilon3 allele increases the risk of Alzheimer's disease and of mild cognitive impairment progressing to Alzheimer's disease. Dement Geriatr Cogn Disord. 2006; 21:81–87. [PubMed: 16340204]

Galvan V, Gorostiza OF, Banwait S, et al. Reversal of Alzheimer's-like pathology and behavior in human APP transgenic mice by mutation of Asp664. Proc Natl Acad Sci U S A. 2006; 103:7130–7135. [PubMed: 16641106]

Grimm MO, Grimm HS, Patzold AJ, et al. Regulation of cholesterol and sphingomyelin metabolism by amyloid-beta and presenilin. Nat Cell Biol. 2005; 7:1118–1123. [PubMed: 16227967]

Guo H, Lai L, Butchbach ME, Lin CL. Human glioma cells and undifferentiated primary astrocytes that express aberrant EAAT2 mRNA inhibit normal EAAT2 protein expression and prevent cell death. Mol Cell Neurosci. 2002; 21:546–560. [PubMed: 12504589]

Guo H, Lai L, Butchbach ME, Stockinger MP, Shan X, Bishop GA, Lin CL. Increased expression of the glial glutamate transporter EAAT2 modulates excitotoxicity and delays the onset but not the outcome of ALS in mice. Hum Mol Genet. 2003; 12:2519–2532. [PubMed: 12915461]

Hardy J, Cowburn R, Barton A, Reynolds G, Lofdahl E, O'Carroll AM, Wester P, Winblad B. Region-specific loss of glutamate innervation in Alzheimer's disease. Neurosci Lett. 1987; 73:77–80. [PubMed: 2882446]

Haugeto O, Ullensvang K, Levy LM, Chaudhry FA, Honore T, Nielsen M, Lehre KP, Danbolt NC. Brain glutamate transporter proteins form homomultimers. J Biol Chem. 1996; 271:27715–27722. [PubMed: 8910364]

Helisalmi S, Vepsalainen S, Koivisto AM, Mannermaa A, Iivonen S, Hiltunen M, Kiviniemi V, Soininen H. Association of CYP46 intron 2 polymorphism in Finnish Alzheimer's disease samples and a global scale summary. J Neurol Neurosurg Psychiatry. 2006; 77:421–422. [PubMed: 16484661]

Jacob CP, Koutsilieri E, Bartl J, et al. Alterations in expression of glutamatergic transporters and receptors in sporadic Alzheimer's disease. J Alzheimers Dis. 2007; 11:97–116. [PubMed: 17361039]

Johansson A, Katzov H, Zetterberg H, et al. Variants of CYP46A1 may interact with age and APOE to influence CSF Abeta42 levels in Alzheimer's disease. Hum Genet. 2004; 114:581–587. [PubMed: 15034781]

Li S, Mallory M, Alford M, Tanaka S, Masliah E. Glutamate transporter alterations in Alzheimer disease are possibly associated with abnormal APP expression. J Neuropathol Exp Neurol. 1997; 56:901–911. [PubMed: 9258260]

Lutjohann D, Breuer O, Ahlborg G, Nennesmo I, Siden A, Diczfalusy U, Bjorkhem I. Cholesterol homeostasis in human brain: evidence for an age-dependent flux of 24S-hydroxycholesterol from the brain into the circulation. Proc Natl Acad Sci U S A. 1996; 93:9799–9804. [PubMed: 8790411]

Lutjohann D, Papassotiropoulos A, Bjorkhem I, et al. Plasma 24S-hydroxycholesterol (cerebrosterol) is increased in Alzheimer and vascular demented patients. J Lipid Res. 2000; 41:195–198. [PubMed: 10681402]

Masliah E, Alford M, DeTeresa R, Mallory M, Hansen L. Deficient glutamate transport is associated with neurodegeneration in Alzheimer's disease. Ann Neurol. 1996; 40:759–766. [PubMed: 8957017]

McGeer EG, Singh EA, McGeer PL. Sodium-dependent glutamate binding in senile dementia. Neurobiol Aging. 1987; 8:219–223. [PubMed: 2885768]

Michikawa M, Gong JS, Fan QW, Sawamura N, Yanagisawa K. A novel action of alzheimer's amyloid beta-protein (Abeta): oligomeric Abeta promotes lipid release. J Neurosci. 2001; 21:7226–7235. [PubMed: 11549733]

Mirra SS, Heyman A, McKeel D, et al. The Consortium to Establish a Registry for Alzheimer's Disease (CERAD). Part II. Standardization of the neuropathologic assessment of Alzheimer's disease. Neurology. 1991; 41:479–486. [PubMed: 2011243]

Mucke L, Masliah E, Yu GQ, et al. High-level neuronal expression of abeta 1–42 in wild-type human amyloid protein precursor transgenic mice: synaptotoxicity without plaque formation. J Neurosci. 2000; 20:4050–4058. [PubMed: 10818140]

Papassotiropoulos A, Lutjohann D, Bagli M, et al. 24S-hydroxycholesterol in cerebrospinal fluid is elevated in early stages of dementia. J Psychiatr Res. 2002; 36:27–32. [PubMed: 11755458]

Papassotiropoulos A, Streffer JR, Tsolaki M, et al. Increased brain beta-amyloid load, phosphorylated tau, and risk of Alzheimer disease associated with an intronic CYP46 polymorphism. Arch Neurol. 2003; 60:29–35. [PubMed: 12533085]

Pike LJ. Rafts defined: a report on the Keystone Symposium on Lipid Rafts and Cell Function. J Lipid Res. 2006; 47:1597–1598. [PubMed: 16645198]

Procter AW, Palmer AM, Francis PT, Lowe SL, Neary D, Murphy E, Doshi R, Bowen DM. Evidence of glutamatergic denervation and possible abnormal metabolism in Alzheimer's disease. J Neurochem. 1988; 50:790–802. [PubMed: 3339353]

Ramirez DM, Andersson S, Russell DW. Neuronal expression and subcellular localization of cholesterol 24-hydroxylase in the mouse brain. J Comp Neurol. 2008; 507:1676–1693. [PubMed: 18241055]

Robinson SR. Changes in the cellular distribution of glutamine synthetase in Alzheimer's disease. J Neurosci Res. 2001; 66:972–980. [PubMed: 11746426]

Rothstein JD, Martin LJ, Kuncl RW. Decreased glutamate transport by the brain and spinal cord in amyotrophic lateral sclerosis. The New England journal of medicine. 1992; 326:1464–1468. [PubMed: 1349424]

Rothstein JD, Van Kammen M, Levey AI, Martin LJ, Kuncl RW. Selective loss of glial glutamate transporter GLT-1 in amyotrophic lateral sclerosis. Annals of Neurology. 1995; 38:73–84. [PubMed: 7611729]

Scott HL, Tannenberg AE, Dodd PR. Variant forms of neuronal glutamate transporter sites in Alzheimer's disease cerebral cortex. J Neurochem. 1995; 64:2193–2202. [PubMed: 7722505]

Shan X, Chang Y, Lin CL. Messenger RNA oxidation is an early event preceding cell death and causes reduced protein expression. FASEB J. 2007; 21:2753–2764. [PubMed: 17496160]

Simpson MD, Royston MC, Deakin JF, Cross AJ, Mann DM, Slater P. Regional changes in [3H]D-aspartate and [3H]TCP binding sites in Alzheimer's disease brains. Brain Res. 1988; 462:76–82. [PubMed: 2846124]

Tian G, Lai L, Guo H, Lin Y, Butchbach ME, Chang Y, Lin CL. Translational control of glial glutamate transporter EAAT2 expression. J Biol Chem. 2007; 282:1727–1737. [PubMed: 17138558]

Trotti D, Danbolt NC, Volterra A. Glutamate transporters are oxidant-vulnerable: a molecular link between oxidative and excitotoxic neurodegeneration? Trends Pharmacol Sci. 1998; 19:328–334. [PubMed: 9745361]

Wang F, Jia J. Polymorphisms of cholesterol metabolism genes CYP46 and ABCA1 and the risk of sporadic Alzheimer's disease in Chinese. Brain Res. 2007; 1147:34–38. [PubMed: 17335784]

Zschocke J, Bayatti N, Behl C. Caveolin and GLT-1 gene expression is reciprocally regulated in primary astrocytes: association of GLT-1 with non-caveolar lipid rafts. Glia. 2005; 49:275–287. [PubMed: 15494979]

Figure 1

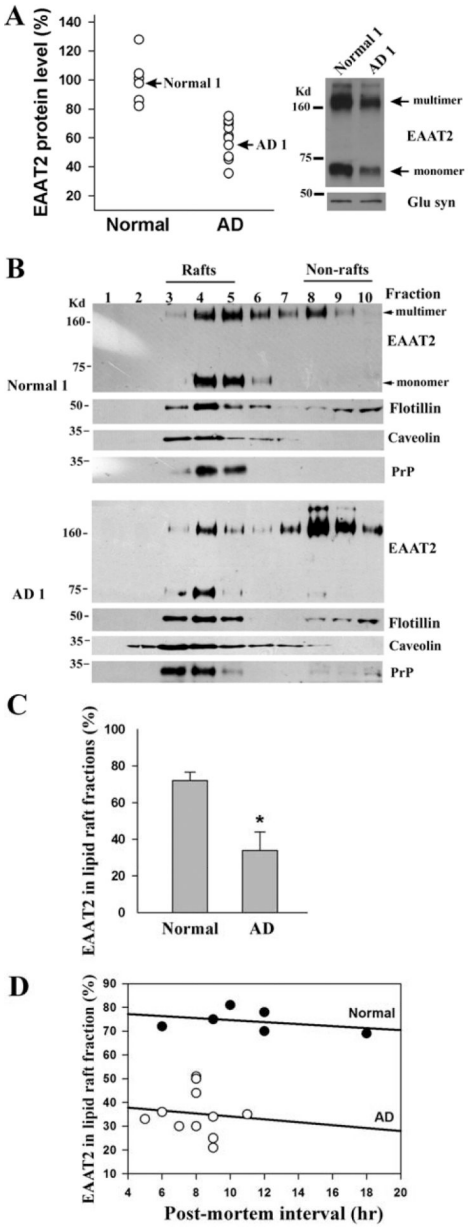

35

Fig. 1.

The association of EAAT2 with lipid rafts is partially disrupted in AD frontal cortices. (**A**) Western blot analysis revealed that total EAAT2 protein levels were significantly decreased in AD tissues (59.9±12.9%; n=11) compared with that in normal tissues (100±15.9%; n=6). EAAT2 protein level for each sample was normalized to glutamine synthetase protein level. (**B**) Western blot analysis of EAAT2 distribution in the lipid raft fractions revealed that most of the EAAT2 proteins from normal control samples (normal 1 sample is shown) were present in the low density fractions (*fractions 3–5, lipid raft fractions*), and most of the EAAT2 proteins from AD samples (AD1 sample is shown) were present in the high density fractions (*fractions 8–10, non-lipid raft fractions*). However, other lipid raft-associated

proteins, flotillin-1, caveolin, and prion protein (PrP), were present primarily in fractions 3–5 in both AD and normal control samples. (**C**) Densitometric quantification analysis revealed that 74.2±4.7% of total EAAT2 signal intensity was associated with lipid raft fractions in normal controls (n=6), but only 35.4±9.6% of total EAAT2 signal intensity was associated with lipid raft fractions in AD frontal cortices (n=11) (**P*<0.001). Both monomeric and multimeric bands were used for analysis. (**D**) Linear regression analysis showed that post-mortem intervals did not affect the amount of EAAT2 protein associated with lipid raft microdomains.

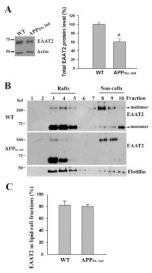

Fig. 2.

EAAT2 proteins are properly associated with lipid rafts in APP transgenic mice. The forebrains of $APP_{Sw,Ind}$ transgenic mice (9-month-old) as well as non-transgenic littermates (n=3 each) were used in this study. (**A**) Western blot analysis of tissue homogenates revealed that there was a 40–50% loss of EAAT2 protein in $APP_{Sw,Ind}$ samples. **P*<0.01 (**B**) Western blot analysis showed that the distribution of EAAT2 in lipid raft and non-lipid raft fraction was similar between APP transgenic and non-transgenic samples. Flotillin-1, a known lipid raft-associated protein, was present primarily in fractions 3–5. (**C**) Densitometric quantification analysis. Both monomeric and multimeric bands were used for analysis. Abnormal APP process and amyloid deposition do not induce the dissociation of EAAT2 from lipid rafts.

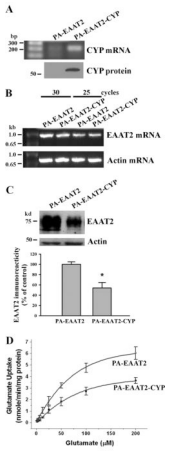

Fig. 3.

Increased expression of CYP46 results in a decrease in EAAT2 protein levels and associated glutamate uptake functions in primary astrocytes. PA-EAAT2 cells stably expressed EAAT2 and PA-EAAT2-CYP cells stably expressed both EAAT2 and CYP46. (**A&B**) Quantitative RT-PCR analysis indicated that PA-EAAT2-CYP cells expressed significantly greater amounts of CYP46 mRNA than that of PA-EAAT2 cells (**A**), but both cell lines expressed similar amounts of EAAT2 mRNA (**B**). (**C**) Western blot analysis showed that PA-EAAT2-CYP cells expressed significantly smaller amounts of EAAT2 protein than that of PA-EAAT2 cells (**P*<0.005). (**D**) [^{3}H]glutamate uptake assay showed that glutamate uptake activity in PA-EAAT2-CYP cells was significantly decreased when compared to that in PA-EAAT2 cells. Increased CYP46 expression caused a decrease in uptake *V*max and an increase in the apparent glutamate *K*m. PA-EAAT2: *V*max = 10.25 nmol/min/mg protein; *K*m = 111.1 μM. PA-EAAT2-CYP: *V*max = 6.89 nmol/min/mg protein; *K*m = 153.6 μM.

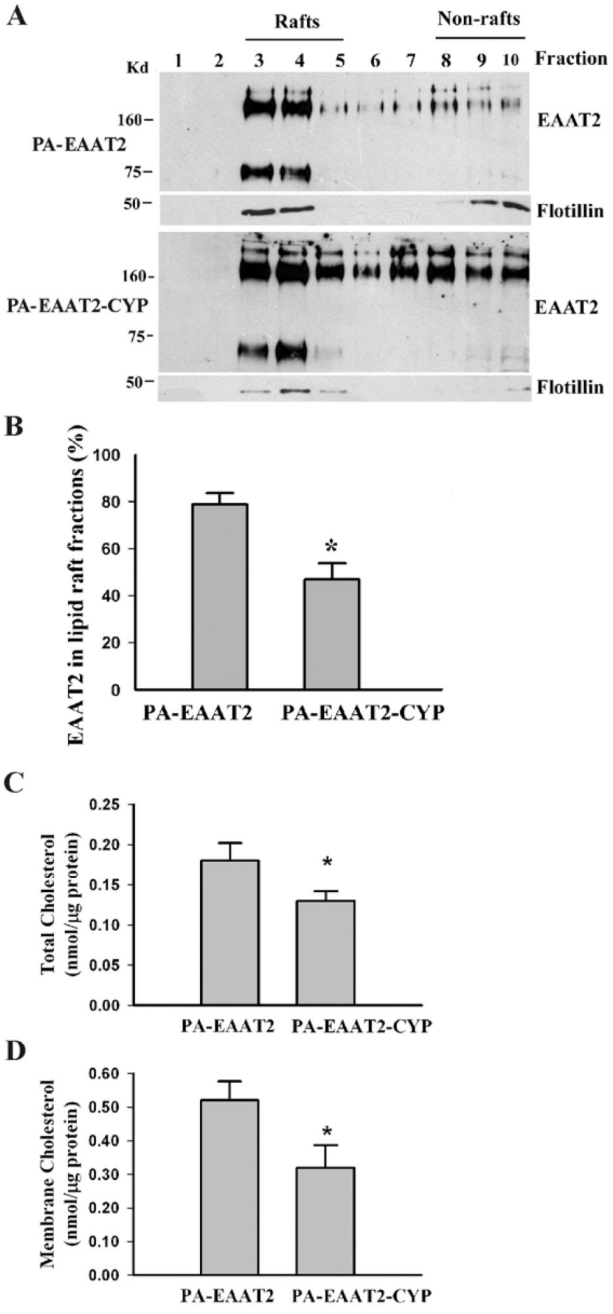

Fig. 4.

Increased expression of CYP46 results in reduction of membrane cholesterol levels and dissociation of EAAT2 from lipid raft microdomains in primary astrocytes. PA-EAAT2 cells stably expressed EAAT2 and PA-EAAT2-CYP cells stably expressed both EAAT2 and CYP46. (**A**) Lipid raft analysis revealed that a significant amount of EAAT2 was moved to the non-lipid raft fractions in PA-EAAT2-CYP cells. (**B**) Densitometric quantification analysis showed a significant reduction in the amount of EAAT2 associated with lipid raft fraction (**P*<0.005). Both monomeric and multimeric bands were used for analysis. (**C&D**) Cholesterol analysis showed that total cholesterol levels (**C**) as well as membrane cholesterol levels (**D**) were significantly decreased in PA-EAAT2-CYP cells when

compared with that in PA-EAAT2 cells (*P<0.05). Three independent experiments were performed with consistent results.

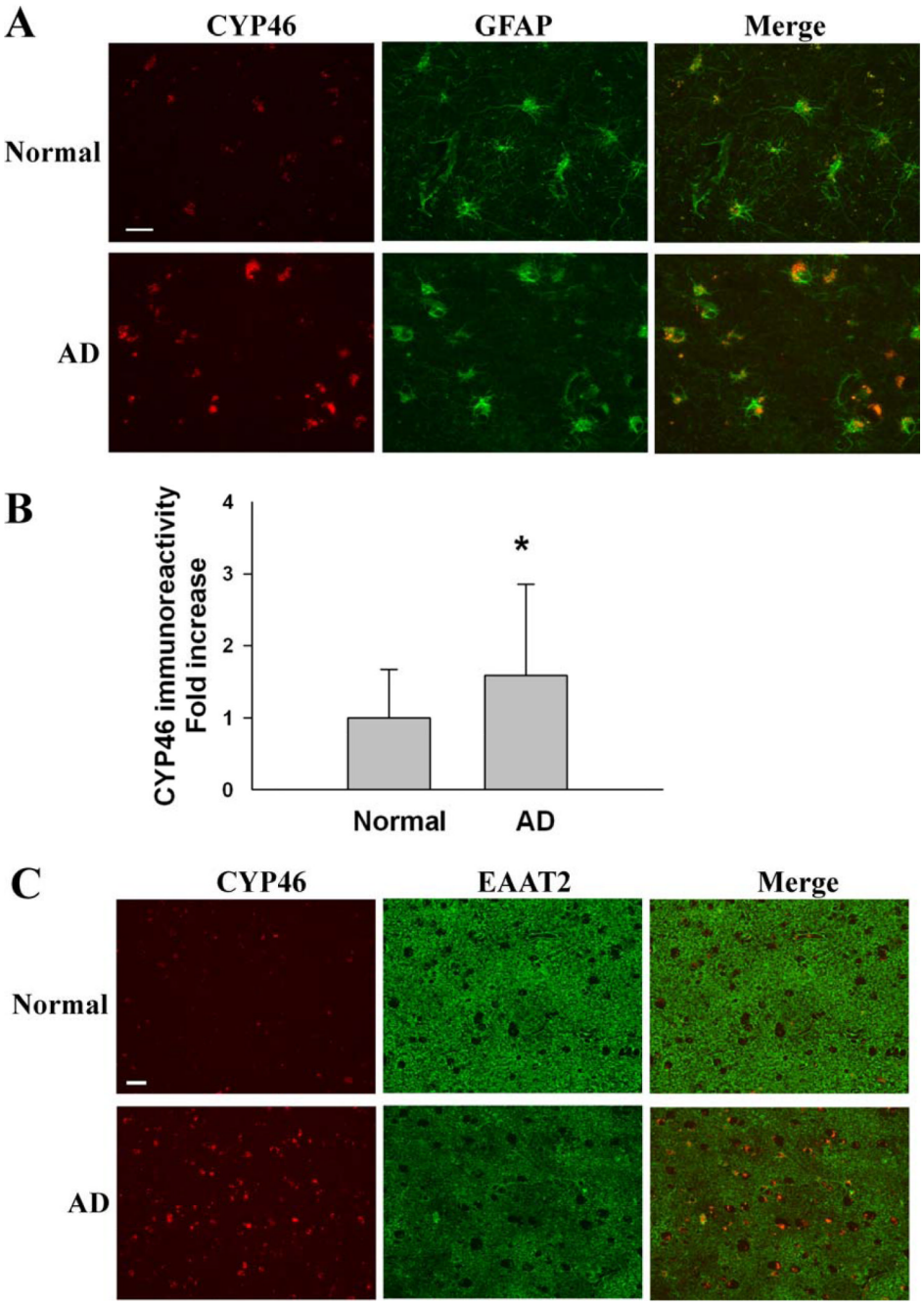

Fig. 5.

Immunohistochemical analysis of CYP46 and EAAT2 in AD frontal cortices. (**A**) A significant increase in CYP46 immunoreactivity in the GFAP-positive astrocytes of AD frontal cortices when compared with normal controls (n=5 each). (**B**) Densitometric quantification analysis revealed a 1.5- to 3- fold increase in CYP46 immunoreactivity in the astrocytes of AD frontal cortices (171 astrocytes) when compared with normal controls (95 astrocytes). **P*<0.01. (**C**) The increase of CYP46 immunoreactivity is concomitant with a focal loss of EAAT2 immunoreactivity in AD frontal cortices. Scale bar, 50 μm.